PHILOSOPHICAL TRANSACTIONS A

royalsocietypublishing.org/journal/rsta

Research

Cite this article: Nizovtseva IG, Alexandrov DV. 2020 The effect of density changes on crystallization with a mushy layer. *Phil. Trans. R. Soc. A* **378**: 20190248.
http://dx.doi.org/10.1098/rsta.2019.0248

Accepted: 30 October 2019

One contribution of 18 to a theme issue 'Patterns in soft and biological matters'.

Subject Areas:
complexity, mathematical modelling, applied mathematics, solid state physics

Keywords:
mushy layer, heat and mass transfer, analytical solutions, phase transformations

Author for correspondence:
Irina G. Nizovtseva
e-mail: nizovtseva.irina@gmail.com

The effect of density changes on crystallization with a mushy layer

Irina G. Nizovtseva[1] and Dmitri V. Alexandrov[2]

[1]Physikalisch-Astronomische Fakultät, Friedrich-Schiller-Universität Jena, Jena 07743, Germany
[2]Department of Theoretical and Mathematical Physics, Laboratory of Multi-Scale Mathematical Modeling, Ural Federal University, Ekaterinburg, 620000, Russian Federation

IGN, 0000-0002-7766-7351; DVA, 0000-0002-6628-745X

A nonlinear problem with two moving boundaries of the phase transition, which describes the process of directional crystallization in the presence of a quasi-equilibrium two-phase layer, is solved analytically for the steady-state process. The exact analytical solution in a two-phase layer is found in a parametric form (the solid phase fraction plays the role of this parameter) with allowance for possible changes in the density of the liquid phase accordingly to a linearized equation of state and arbitrary value of the solid fraction at the boundary between the two-phase and solid layers. Namely, the solute concentration, temperature, solid fraction in the mushy layer, liquid and solid phases, mushy layer thickness and its velocity are found analytically. The theory under consideration is in good agreement with experimental data. The obtained solutions have great potential applications in analysing similar processes with a two-phase layer met in materials science, geophysics, biophysics and medical physics, where the directional crystallization processes with a quasi-equilibrium mushy layer can occur.

This article is part of the theme issue 'Patterns in soft and biological matters'.

1. Introduction

The phase transition processes in the presence of a two-phase solid/liquid layer frequently occur in a large variety of applied problems ranging from solidification in materials science, chemical industry and geophysics (e.g. crystallization of sea ices, lava

THE ROYAL SOCIETY PUBLISHING

lakes and at the Earth's inner core) to crystallization in biophysics and medical physics (e.g. biocrystallization and crystallization of proteins and DNA complexes) [1–13]. A two-phase layer lying between solid and liquid substances is filled with the liquid phase and growing solid structures. This layer moves in the direction of increasing temperature and its time-dependent coordinates and velocity should be found from the solution of the moving boundary problem. The first theoretical models of the two-phase (mushy) layer were developed by Hills, Loper, Roberts, Fowler and Borisov in the 1980s [14–17]. Note that a complete theoretical description of such a process is complicated by the presence of different physical mechanisms such as dendritic growth and nucleation of crystals, buoyancy and gravitational forces, solute impurities, coarsening kinetics, joule heating, convective and hydrodynamic flows etc. (see, among others, [18–32]).

In the present paper, a new analytical approach for solving a nonlinear heat and mass transfer equations in a two-phase layer is developed in the steady-state crystallization conditions with allowance for the temperature- and concentration-dependent density in liquid. This approach extends previously known analytical solutions of mushy layer equations for the steady-state solidification regime [33,34] and enables us to describe a wider class of crystallization problems met in applied science. The theory under consideration can be used for the description of directional solidification processes of binary melts and solutions with a mushy layer in materials science, geophysics, biophysics and medical physics taking into account the temperature- and concentration-dependent density in liquid.

2. The model

Let us consider the process of directional solidification along the spatial coordinate ξ (figure 1). The solid phase/mushy layer phase boundary is $\Sigma(\tau)$ whereas the mushy layer/liquid phase boundary is $\Sigma(\tau)+\delta$, where τ and δ represent the time and two-phase layer thickness. The solid material, two-phase layer and liquid phase are, respectively, located in regions $\xi<\Sigma(\tau)$, $\Sigma(\tau)<\xi<\Sigma(\tau)+\delta$ and $\xi>\Sigma(\tau)+\delta$. The heat and mass transfer equations in the two-phase layer can be written as (see, among others, [14–16,33–36])

$$\left.\begin{aligned}&\rho_m C_m\frac{\partial\theta_m}{\partial\tau}=\frac{\partial}{\partial\xi}\left(\lambda_m\frac{\partial\theta_m}{\partial\xi}\right)+L_V\frac{\partial\varphi}{\partial\tau}\\ \text{and}\quad&\theta_m=\theta_L(\sigma_0)+\Gamma(\sigma_m-\sigma_0),\ \ \Sigma(\tau)<\xi<\Sigma(\tau)+\delta,\end{aligned}\right\}\tag{2.1}$$

$$\frac{\partial}{\partial\tau}\left[(1-\varphi)\sigma_m\right]=\frac{\partial}{\partial\xi}\left(D_m\frac{\partial\sigma_m}{\partial\xi}\right)-k\sigma_m\frac{\partial\varphi}{\partial\tau},\ \ \Sigma(\tau)<\xi<\Sigma(\tau)+\delta,\tag{2.2}$$

where θ_m and σ_m are the temperature and solute concentration in the two-phase layer, φ is the fraction of solid phase, L_V is the latent heat parameter, σ_0 is a reference value of the solute concentration in liquid, θ_L is the liquidus temperature, Γ is the slope of the liquidus line, k is the equilibrium segregation coefficient, and the density ρ_m, heat capacity C_m, thermal conductivity λ_m and diffusion coefficient D_m in the two-phase layer can be expressed as volume-fraction-weighted averages of the properties of liquid and solid [37]

$$\rho_m C_m=\rho_l C_l(1-\varphi)+\rho_s C_s\varphi,\quad \lambda_m=\lambda_l(1-\varphi)+\lambda_s\varphi\qquad\text{and}\quad D_m=D_l(1-\varphi),\tag{2.3}$$

where we traditionally neglect diffusion in the solid phase. Here, ρ_l and ρ_s are the densities in the liquid and solid phases, C_l and C_s are the heat capacities in these phases, λ_l and λ_s are the thermal conductivities in liquid and solid, and D_l represents the diffusion coefficient in liquid.

The density of the fluid changes accordingly to a linearized equation of state

$$\rho_l=\rho_0\{1-\alpha^*\left[\theta_m-\theta_L(\sigma_0)\right]+\beta^*\left(\sigma_m-\sigma_0\right)\},\tag{2.4}$$

where ρ_0 is a reference density, α^* and β^* are the constant expansion coefficients for heat and solute.

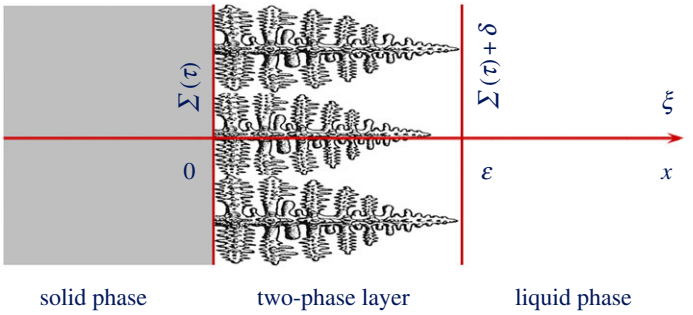

Figure 1. Schematic illustration of the directional solidification process with a two-phase layer where the growing solid phase in the form of dendrite-like structures is shown. (Online version in colour.)

The boundary conditions at the solid phase/two-phase layer (at $\xi = \Sigma(\tau)$) and two-phase layer/liquid phase (at $\xi = \Sigma(\tau) + \delta$) boundaries have the form [33–36]

$$\left.\begin{aligned} &\lambda_s \frac{\partial \theta_s}{\partial \xi} - \lambda_m \frac{\partial \theta_m}{\partial \xi} = L_V(1-\varphi_*)\frac{\mathrm{d}\Sigma}{\mathrm{d}\tau} \\ \text{and}\quad &(1-k)(1-\varphi_*)\sigma_m \frac{\mathrm{d}\Sigma}{\mathrm{d}\tau} + D_m \frac{\partial \sigma_m}{\partial \xi} = 0,\ \varphi = \varphi_*,\ \xi = \Sigma(\tau), \end{aligned}\right\} \tag{2.5}$$

$$\sigma_m = \sigma_l,\ \frac{\partial \sigma_m}{\partial \xi} = \frac{\partial \sigma_l}{\partial \xi},\ \frac{\partial \theta_m}{\partial \xi} = \frac{\partial \theta_l}{\partial \xi},\ \varphi = 0,\ \xi = \Sigma(\tau) + \delta, \tag{2.6}$$

where θ_s and θ_l represent the temperatures in the solid and liquid phases, φ_* is the solid fraction at the solid phase/two-phase layer boundary, and σ_l is the solute concentration in liquid.

We consider the solidification process at fixed temperature gradients. In this case, the temperature and concentration fields in the solid (at $\xi < \Sigma(\tau)$) and liquid (at $\xi > \Sigma(\tau) + \delta$) phases are described by equations

$$\frac{\partial \theta_s}{\partial \xi} = g_s,\ \xi < \Sigma(\tau);\ \frac{\partial \theta_l}{\partial \xi} = g_l,\ \frac{\partial \sigma_l}{\partial \tau} = D_l \frac{\partial^2 \sigma_l}{\partial \xi^2},\ \xi > \Sigma(\tau) + \delta;\ \sigma_l \to \sigma_0,\ \xi \to \infty, \tag{2.7}$$

where g_s and g_l represent the constant temperature gradients in the solid and liquid phases and the two-phase layer thickness does not depend on time [31,32,38].

The model (2.1)–(2.7) is the nonlinear model with two moving boundaries of the phase transition. Note that there are no general methods for solving such models. Below we consider how to find the exact analytical solution of equations (2.1)–(2.7) in the case of steady-state solidification with a constant velocity $\mathrm{d}\Sigma/\mathrm{d}\tau = u_s$, which must be determined from the solution of the problem.

3. Analytical solution

For the sake of convenience, let us introduce the following dimensionless variables and parameters

$$\left.\begin{aligned} &x = \frac{u_s}{D_l}(\xi - u_s\tau),\ c_m = \frac{\sigma_m}{\sigma_0},\ c_l = \frac{\sigma_l}{\sigma_0},\ T_m = \frac{\theta_m}{m\sigma_0},\ \Lambda_0(\varphi) = \frac{\lambda_m(\varphi)}{\lambda_s}, \\ &\tilde{\beta} = \left(\beta^* + m\alpha^*\right)\sigma_0,\ R = \frac{\rho_s C_s}{\rho_0 C_l},\ m = -\Gamma,\ T_0 = \frac{\theta_0}{m\sigma_0},\ \theta_0 = \theta_L(\sigma_0) - \Gamma\sigma_0, \\ &a_1 = \frac{\lambda_s}{\rho_0 C_l D_l},\ a_2 = \frac{L_V}{\rho_0 C_l m\sigma_0},\ \tilde{L}_V = \frac{L_V D_l}{\lambda_s m\sigma_0},\ G_s = \frac{g_s D_l}{u_s m\sigma_0},\ G_l = \frac{g_l D_l}{u_s m\sigma_0} \\ \text{and}\quad &\varepsilon = \frac{u_s\delta}{D_l},\ g(c_m,\varphi) = \left[1 + \tilde{\beta}(c_m - 1)\right](1-\varphi) + R\varphi. \end{aligned}\right\} \tag{3.1}$$

The nonlinear model (2.1)–(2.7) in dimensionless variables (3.1) takes the form

$$g(c_m,\varphi)\frac{\mathrm{d}c_m}{\mathrm{d}x}+a_1\frac{\mathrm{d}}{\mathrm{d}x}\left[\Lambda_0(\varphi)\frac{\mathrm{d}c_m}{\mathrm{d}x}\right]+a_2\frac{\mathrm{d}\varphi}{\mathrm{d}x}=0,\ T_m=T_0-c_m,\ 0<x<\varepsilon, \tag{3.2}$$

$$\frac{\mathrm{d}}{\mathrm{d}x}\left[(1-\varphi)c_m\right]+\frac{\mathrm{d}}{\mathrm{d}x}\left[(1-\varphi)\frac{\mathrm{d}c_m}{\mathrm{d}x}\right]+kc_m\frac{\mathrm{d}\varphi}{\mathrm{d}x}=0,\ 0<x<\varepsilon, \tag{3.3}$$

$$G_s+\Lambda_0(\varphi_*)\frac{\mathrm{d}c_m}{\mathrm{d}x}=\tilde{L}_V(1-\varphi_*),\ \varphi=\varphi_*,\ x=0, \tag{3.4}$$

$$(1-k)c_m+\frac{\mathrm{d}c_m}{\mathrm{d}x}=0,\ x=0 \text{ if } \varphi_*\neq 1, \text{ otherwise } \varphi_*=1,\ x=0, \tag{3.5}$$

$$c_m=c_l,\ \frac{\mathrm{d}c_m}{\mathrm{d}x}=\frac{\mathrm{d}c_l}{\mathrm{d}x}=-G_l,\ \varphi=0,\ x=\varepsilon \tag{3.6}$$

and

$$\frac{\mathrm{d}^2c_l}{\mathrm{d}x^2}+\frac{\mathrm{d}c_l}{\mathrm{d}x}=0,\ x>\varepsilon \text{ and } c_l\to 1,\ x\to\infty. \tag{3.7}$$

After integration of the first equation (3.7), we can easily find the concentration distribution in the liquid phase (at $x>\varepsilon$). Using the third boundary condition (3.6) and the last expression (3.7), we finally obtain

$$c_l(x)=1+G_l\exp(\varepsilon-x),\quad x>\varepsilon. \tag{3.8}$$

In order to determine the concentration field in the two-phase layer (at $0<x<\varepsilon$), let us express the concentration derivative $\mathrm{d}c_m/\mathrm{d}x=c_{mx}$ from equations (3.2) and (3.3) as

$$\frac{\mathrm{d}c_m}{\mathrm{d}x}=c_{mx}=\frac{\left[f_1(\varphi)-f_2(\varphi)c_m\right]\mathrm{d}c_m/\mathrm{d}\varphi-f_3(\varphi)-f_4(\varphi)c_m}{f_5(\varphi)},\ 0<x<\varepsilon, \tag{3.9}$$

where

$$f_1(\varphi)=(1-\varphi)\left[a_1\Lambda_0(\varphi)+\left(\tilde{\beta}-1\right)(1-\varphi)-R\varphi\right],\ f_2(\varphi)=\tilde{\beta}(1-\varphi)^2,$$

and

$$f_3(\varphi)=a_2(1-\varphi),\ f_4(\varphi)=(1-k)a_1\Lambda_0(\varphi),\ f_5(\varphi)=a_1\left[(1-\varphi)\frac{\mathrm{d}\Lambda_0}{\mathrm{d}\varphi}+\Lambda_0(\varphi)\right].$$

Now substituting $\mathrm{d}c_m/\mathrm{d}x$ from (3.9) into equation (3.3), we come to the following Cauchy problem for concentration c_m as a function of φ in the two-phase layer ($c_m'=\mathrm{d}c_m/\mathrm{d}\varphi$, $\mathrm{d}f_5/\mathrm{d}\varphi=0$)

$$\frac{\mathrm{d}^2c_m}{\mathrm{d}\varphi^2}=\frac{F(c_m',c_m,\varphi)f_5(\varphi)-(1-\varphi)h_1(c_m',c_m,\varphi)}{(1-\varphi)h_2(c_m,\varphi)} \tag{3.10}$$

and

$$c_m=1+G_l,\ \text{and}\ \frac{\mathrm{d}c_m}{\mathrm{d}\varphi}=\frac{f_3(0)+(1+G_l)f_4(0)-G_lf_5(0)}{f_1(0)-(1+G_l)f_2(0)},\ \varphi=0, \tag{3.11}$$

where

$$h_1(c_m',c_m,\varphi)=\left[f_1'(\varphi)-f_2'(\varphi)c_m-f_2(\varphi)c_m'\right]c_m'-f_3'(\varphi)-f_4'(\varphi)c_m-f_4(\varphi)c_m'$$

and

$$h_2(c_m,\varphi)=f_1(\varphi)-f_2(\varphi)c_m,\ F(c_m',c_m,\varphi)=(1-k)c_m-(1-\varphi)c_m'+c_{mx}(c_m',c_m,\varphi),$$

and expressions (3.6), (3.8) and (3.9) have been used.

If $\varphi_*\neq 1$, one can determine the following expression for φ_* from the boundary conditions (3.4) and (3.5)

$$c_m(\varphi_*)=\frac{G_s-\tilde{L}_V(1-\varphi_*)}{(1-k)\Lambda_0(\varphi_*)}, \tag{3.12}$$

where $c_m(\varphi_*)$ must be found from the solution of Cauchy problem (3.10), (3.11). The first expression (3.5) in this case defines u_s from the equation $(1-k)c_m(\varphi_*)+c_{mx}(\varphi_*)=0$, where c_{mx} is determined in (3.9). In the opposite case, when $\varphi_*=1$, the boundary condition (3.4) determines the steady-state velocity u_s.

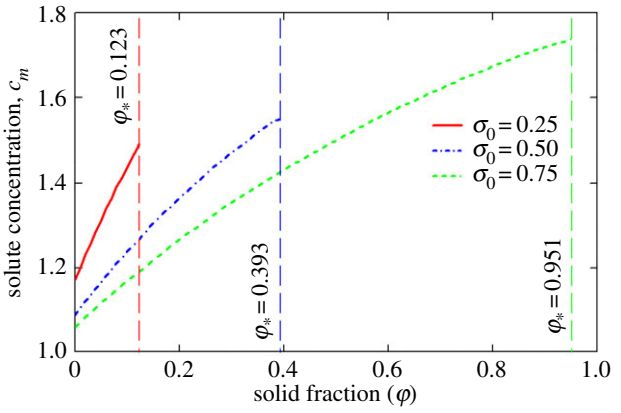

Figure 2. The solute concentration as a function of the solid fraction in the two-phase layer. The vertical lines show the solid phase/two-phase layer boundary where $\varphi = \varphi_*$. Parameters used for calculations (Fe–Ni alloy) are $\lambda_l/\lambda_s = 0.565$, $\tilde{\beta} = 0.75$, $\tilde{L}_V = 0.538$, $R = 0.623$, $k = 0.68$, $a_1 = 4958$, $a_2 = 2.669$, $G_l = 0.057$ and $G_s = 0.57$. (Online version in colour.)

Now taking into account that $\mathrm{d}c_m/\mathrm{d}x = (\mathrm{d}c_m/\mathrm{d}\varphi)(\mathrm{d}\varphi/\mathrm{d}x)$, we arrive at the following explicit solutions for the dimensionless thickness of two-phase layer ε and $x(\varphi)$

$$\varepsilon = -\int_0^{\varphi_*} \frac{\mathrm{d}c_m/\mathrm{d}\varphi_1}{c_{mx}(\varphi_1)}\mathrm{d}\varphi_1 \quad \text{and} \quad x(\varphi) = \varepsilon + \int_0^{\varphi} \frac{\mathrm{d}c_m/\mathrm{d}\varphi_1}{c_{mx}(\varphi_1)}\,\mathrm{d}\varphi_1, \tag{3.13}$$

where again $c_{mx}(\varphi_1)$ and $\mathrm{d}c_m/\mathrm{d}\varphi_1$ are determined by expressions (3.9)–(3.11).

Thus, a complete analytical solution in the two-phase layer, (3.9)–(3.13), is found in a parametric form (with parameter φ).

4. Conclusion

The obtained analytical solution for the solute concentration in the two-phase and liquid layers is illustrated in figures 2–4. Note that the temperature field in the mixed layer is also determined in accordance with the second expression (3.2) whereas in the solid and liquid layers it is defined by the constant temperature gradients (see equations (2.7)). Figures 2 and 3 show the solute concentration c_m and spatial coordinate x as functions of the solid fraction φ accordingly to exact analytical solutions (3.10), (3.11) and (3.13). Let us emphasize that the solute concentration increases with increasing φ (decreasing x), i.e. c_m attains its maximum at the boundary between the solid and two-phase layers (at $\varphi = \varphi_*$).

The parametric solutions $c_m(\varphi)$ and $x(\varphi)$ in the two-phase layer enable us to find the solute concentration c_m as a function of the spatial coordinate x. This dependence is shown in figure 4 on the left-hand side of the corresponding vertical line plotted for a certain initial concentration σ_0. The concentration c_l in the liquid region shown in figure 4 by the dotted lines on the right-hand side of each vertical line is demonstrated accordingly to expression (3.8). Note that the concentration profiles $c_m(x)$ and $c_l(x)$ coincide at the two-phase layer/liquid phase boundary and determine the thickness ε of the two-phase region. The greater values of initial concentration σ_0 increase the two-phase layer thickness ε and the solid fraction φ_* at the solid phase/two-phase layer boundary. The interfacial concentration $\sigma_s = k\sigma_0 c_m$ determined on the left-hand side of the boundary solid phase/two-phase layer enables us to obtain the concentration distribution in the solid phase appearing as a result of impurity absorption by the solid phase at $x = 0$. Thus, the obtained solutions completely describe the concentration and temperature profiles, the solid phase distribution as well as the steady-state velocity of the two-phase layer and its thickness.

Figure 5 compares the impurity concentration in the solid phase calculated accordingly to the theory under consideration and experimental data [39] for a set of KCl crystals. It is easily seen that the theory well agrees with experiments. An important point is that the present analytical

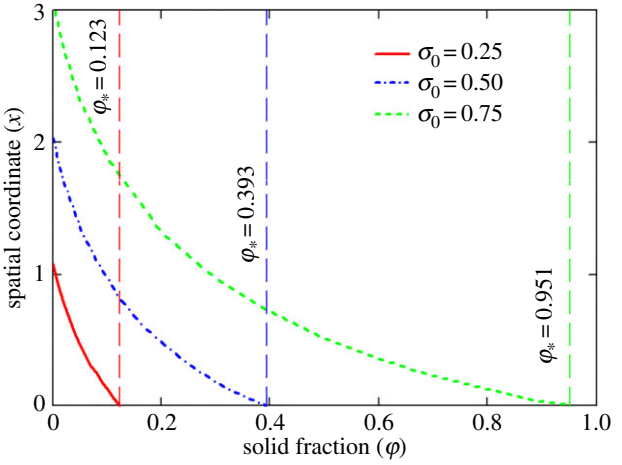

Figure 3. The spatial coordinate as a function of the solid fraction in the two-phase layer. The vertical lines show the solid phase/two-phase layer boundary where $\varphi = \varphi_*$ and $x = 0$. (Online version in colour.)

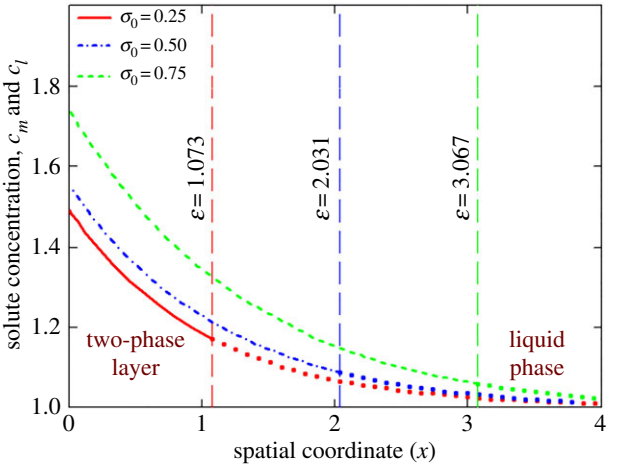

Figure 4. The solute concentration as a function of the spatial coordinate in the two-phase and liquid layers. The vertical lines show the boundary between the two-phase and liquid layers. The profile of solute concentration c_l in the liquid layer (dots) lies on the right-hand side of the vertical line plotted for a certain concentration σ_0. (Online version in colour.)

solution transforms to the previously known steady-state solutions [33,34] in the limiting case of constant density in the liquid phase, i.e. if $\alpha^* = \beta^* = 0$, and $\rho_l = \rho_0 = \text{const}$.

In summary, the theory under consideration shows how to construct an exact analytical solution of nonlinear phase transition problem in the presence of a mixed layer where the solid and liquid phases coexist together and their fractions must be determined from the solution of the moving boundary problem. Note that the general methods for solving such nonlinear heat and mass transfer problems with two moving boundaries are unknown. Within the framework of the formulated heat and mass transfer equations, the developed theory contains no limitations and can be applied to the description of various processes of steady-state crystallization. The theory takes into account possible variations of the density of the liquid phase accordingly to a linearized equation of state and arbitrary value of the solid phase fraction at the boundary between the two-phase and solid layers. The present analytical approach can be used for solving similar problems arising in geophysics, biophysics, medical physics and materials science, where a quasi-equilibrium crystallization with a mushy layer can occur.

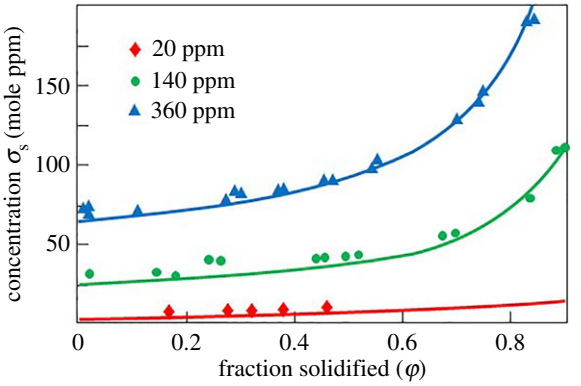

Figure 5. Theoretical predictions (solid lines) and experimental data [39] (symbols) for a set of KCl crystals doped with $c_0 = 20$, 140 and 360 mole ppm of divalent europium, $c_0 = \sigma_0(1 + G_l)$, $k = 0.18$, $\alpha^* = 0$ and $\beta^* = 0$. (Online version in colour.)

Let us especially note in conclusion that the present analysis can be extended to the case of weakly non-equilibrium mushy layer crystallization (where nucleation and growth of crystals occur in a metastable liquid) in the spirit of previously developed theories [40,41]. A step forward for future research will also be the development of a theory of non-stationary crystallization with a two-phase zone, taking into account the temperature and concentration dependence of the density of the liquid phase, by analogy with the previous theories [42,43].

Data accessibility. This article does not contain any additional data.

Authors' contributions. All authors contributed equally to this study.

Competing interests. We declare we have no competing interests.

Funding. This work was supported by the Russian Science Foundation (grant no. 18-19-00008).

References

1. Huppert HE, Worster MG. 1985 Dynamic solidification of a binary melt. *Nature* **314**, 703–707. (doi:10.1038/314703a0)
2. Kurz W, Fisher DJ. 1989 *Fundamentals of solidification*. Aedermannsdorf: Trans Tech Publications.
3. Alexandrov DV, Malygin AP, Alexandrova IV. 2006 Solidification of leads: approximate solutions of non-linear problem. *Ann. Glaciol.* **44**, 118–122. (doi:10.3189/172756406781811213)
4. Barlow DA. 2009 Theory of the intermediate stage of crystal growth with applications to protein crystallization. *J. Cryst. Growth* **311**, 2480–2483. (doi:10.1016/j.jcrysgro.2009.02.035)
5. Alexandrov DV, Netreba AV, Malygin AP. 2012 Time-dependent crystallization in magma chambers and lava lakes cooled from above: the role of convection and kinetics on nonlinear dynamics of binary systems. *Int. J. Heat Mass Trans.* **55**, 1189–1196. (doi:10.1016/j.ijheatmasstransfer.2011.09.048)
6. Ivanov AA, Alexandrov DV, Alexandrova IV. 2020 Dissolution of polydisperse ensembles of crystals in channels with a forced flow. *Phil. Trans. R. Soc. A* **378**, 20190246. (doi:10.1098/rsta.2019.0246)
7. Jones DWR, Worster MG. 2013 Fluxes through steady chimneys in a mushy layer during binary alloy solidification. *J. Fluid Mech.* **714**, 127–151. (doi:10.1017/jfm.2012.462)
8. Huguet L, Alboussière T, Bergman MI, Deguen R, Labrosse S, Lesoeur G. 2016 Structure of a mushy layer under hypergravity with implications for Earth's inner core. *Geophys. J. Int.* **204**, 1729–1755. (doi:10.1093/gji/ggv554)
9. Alexandrov DV, Bashkirtseva IA, Ryashko LB. 2018 Nonlinear dynamics of mushy layers induced by external stochastic fluctuations. *Phil. Trans. R. Soc. A* **376**, 20170216. (doi:10.1098/rsta.2017.0216)
10. Galenko PK, Alexandrov DV. 2018 From atomistic interfaces to dendritic patterns. *Phil. Trans. R. Soc. A* **376**, 20170210. (doi:10.1098/rsta.2017.0210)

11. Alexandrov DV, Nizovtseva IG. 2019 On the theory of crystal growth in metastable systems with biomedical applications: protein and insulin crystallization. *Phil. Trans. R. Soc. A* **377**, 20180214. (doi:10.1098/rsta.2018.0214)
12. Alexandrova IV, Alexandrov DV. 2020 Dynamics of particulate assemblages in metastable liquids: a test of theory with nucleation and growth kinetics. *Phil. Trans. R. Soc. A* **378**, 20190245. (doi:10.1098/rsta.2019.0245)
13. Alexandrov DV, Alexandrova IV. 2020 From nucleation and coarsening to coalescence in metastable liquids. *Phil. Trans. R. Soc. A* **378**, 20190247. (doi:10.1098/rsta.2019.0247)
14. Hills RN, Loper DE, Roberts PH. 1983 A thermodynamically consistent model of a mushy zone. *Q. J. Appl. Maths.* **36**, 505–539. (doi:10.1093/qjmam/36.4.505)
15. Fowler AC. 1985 The formation of freckles in binary alloys. *IMA J. Appl. Math.* **35**, 159–174. (doi:10.1093/imamat/35.2.159)
16. Borisov VT. 1987 *Theory of two-phase zone of a metal ingot*. Moscow: Metallurgiya Publishing House.
17. Hills RN. 1988 A generalized Scheil-Pfann equation for a dynamical theory of a mushy zone. *Int. J. Non-Linear Mech.* **23**, 327–339. (doi:10.1016/0020-7462(88)90029-7)
18. Martin S, Kauffman P. 1974 The evolution of under-ice melt ponds, or double diffusion at the freezing point. *J. Fluid Mech.* **64**, 507–528. (doi:10.1017/S0022112074002527)
19. Alexandrov DV, Nizovtseva IG. 2008 To the theory of underwater ice evolution, or nonlinear dynamics of 'false bottoms'. *Int. J. Heat Mass Trans.* **51**, 5204–5208. (doi:10.1016/j.ijheatmasstransfer.2007.11.061)
20. Huppert HE. 1990 The fluid mechanics of solidification. *J. Fluid Mech.* **212**, 209–240. (doi:10.1017/S0022112090001938)
21. Hills RN, Roberts PH. 1997 Microstructural coarsening kinetics for a mushy zone of a pure material. *Int. J. Non-Linear Mech.* **32**, 1003–1013. (doi:10.1016/S0020-7462(96)00142-4)
22. Riahi DN. 2012 On non-linear magneto convection in a mushy layer with joule heating. *Int. J. Non-Linear Mech.* **47**, 49–54. (doi:10.1016/j.ijnonlinmec.2012.02.003)
23. Herlach D, Galenko P, Holland-Moritz D. 2007 *Metastable solids from undercooled melts*. Amsterdam, The Netherlands: Elsevier.
24. Alexandrov DV, Malygin AP. 2012 Flow-induced morphological instability and solidification with the slurry and mushy layers in the presence of convection. *Int. J. Heat Mass Trans.* **55**, 3196–3204. (doi:10.1016/j.ijheatmasstransfer.2012.02.048)
25. Qi XB, Chen Y, Kang XH, Li DZ, Gong TZ. 2017 Modeling of coupled motion and growth interaction of equiaxed dendritic crystals in a binary alloy during solidification. *Sci. Rep.* **7**, 45770. (doi:10.1038/srep45770)
26. Alexandrov DV, Ivanov AA, Alexandrova IV. 2018 Analytical solutions of mushy layer equations describing directional solidification in the presence of nucleation. *Phil. Trans. R. Soc. A* **376**, 20170217. (doi:10.1098/rsta.2017.0217)
27. Makoveeva EV, Alexandrov DV. 2018 A complete analytical solution of the Fokker-Planck and balance equations for nucleation and growth of crystals. *Phil. Trans. R. Soc. A* **376**, 20170327. (doi:10.1098/rsta.2017.0327)
28. Galenko PK, Alexandrov DV, Titova EA. 2018 The boundary integral theory for slow and rapid curved solid/liquid interfaces propagating into binary systems. *Phil. Trans. R. Soc. A* **376**, 20170218. (doi:10.1098/rsta.2017.0218)
29. Alexandrov DV, Galenko PK, Toropova LV. 2018 Thermo-solutal and kinetic modes of stable dendritic growth with different symmetries of crystalline anisotropy in the presence of convection. *Phil. Trans. R. Soc. A* **376**, 20170215. (doi:10.1098/rsta.2017.0215)
30. Kerr RC, Woods AW, Worster MG, Huppert HE. 1990 Solidification of an alloy cooled from above Part 1. Equilibrium growth. *J. Fluid Mech.* **216**, 323–342. (doi:10.1017/S0022112090000453)
31. Peppin SSL, Aussillous P, Huppert HE, Worster MG. 2007 Steady-state mushy layers: experiments and theory. *J. Fluid Mech.* **570**, 69–77. (doi:10.1017/S0022112006003028)
32. Peppin SSL, Huppert HE, Worster MG. 2008 Steady-state solidification of aqueous ammonium chloride. *J. Fluid Mech.* **599**, 465–476. (doi:10.1017/S0022112008000219)
33. Alexandrov DV. 2001 Solidification with a quasiequilibrium mushy region: exact analytical solution of nonlinear model. *J. Cryst. Growth* **222**, 816–821. (doi:10.1016/S0022-0248(00)00960-X)

34. Alexandrov DV. 2001 Solidification with a quasiequilibrium two-phase zone. *Acta Mater.* **49**, 759–764. (doi:10.1016/S1359-6454(00)00388-8)
35. Alexandrov DV, Aseev DL. 2005 One-dimensional solidification of an alloy with a mushy zone: thermodiffusion and temperature-dependent diffusivity. *J. Fluid Mech.* **527**, 57–66. (doi:10.1017/S0022112004003052)
36. Alexandrov DV, Malygin AP. 2006 Self-similar solidification of an alloy from a cooled boundary. *Int. J. Heat Mass Trans.* **49**, 763–769. (doi:10.1016/j.ijheatmasstransfer.2005.07.047)
37. Batchelor GK. 1974 Transport properties of two-phase materials with random structure. *Annu. Rev. Fluid Mech.* **6**, 227–255. (doi:10.1146/annurev.fl.06.010174.001303)
38. Buyevich YuA, Iskakova LY, Mansurov VV. 1990 The nonlinear dynamics of solidification of a binary melt with a quasi-equilibrium mushy region. *Can. J. Phys.* **68**, 790–793. (doi:10.1139/p90-115)
39. Czapelski M. 1998 Variable equilibrium partition coefficient. *J. Cryst. Growth* **187**, 138–139. (doi:10.1016/S0022-0248(97)00852-X)
40. Aseev DL, Alexandrov DV. 2006 Directional solidification of binary melts with a non-equilibrium mushy layer. *Int. J. Heat Mass Trans.* **49**, 4903–4909. (doi:10.1016/j.ijheatmasstransfer.2006.05.046)
41. Alexandrov DV, Malygin AP. 2011 Coupled convective and morphological instability of the inner core boundary of the Earth. *Phys. Earth Planet. Inter.* **189**, 134–141. (doi:10.1016/j.pepi.2011.08.004)
42. Alexandrov DV, Aseev DL, Nizovtseva IG, Huang H-N, Lee D. 2007 Nonlinear dynamics of directional solidification with a mushy layer. Analytic solutions of the problem. *Int. J. Heat Mass Trans.* **50**, 3616–3623. (doi:10.1016/j.ijheatmasstransfer.2007.02.006)
43. Alexandrov DV, Nizovtseva IG, Malygin AP, Huang H-N, Lee D. 2008 Unidirectional solidification of binary melts from a cooled boundary: analytical solutions of a nonlinear diffusion-limited problem. *J. Phys.: Condens. Matter* **20**, 114105. (doi:10.1088/0953-8984/20/11/114105)